Water Air Soil Pollut (2021) 232: 150
https://doi.org/10.1007/s11270-021-05107-1

Assessment of Acid Sulfate Drainage in an Environmental Liability Associated with an Ancient Sulfuric Acid Industry in a Sector of the Río de la Plata Coastal Plain: Impacts On Soil And Water Quality

Germán Albiero · Lucía Santucci · Eleonora Carol

Received: 11 December 2020 / Accepted: 31 March 2021 / Published online: 11 April 2021

Abstract Environmental liabilities have become one of the most important problems at environmental level, especially those located in urban areas. Within the area of the Río de la Plata coastal plain, industrial waste abandoned by an ancient sulfuric acid industry in a sector of the petrochemical center constitutes an environmental liability composed mainly of fragments of native sulfur. The aim of this work is to evaluate, from laboratory tests, the generation of sulfate acid drainage in environmental liabilities associated with the ancient sulfuric acid industry in order to identify the waste spatial distribution and to determine the impacts that they impart on the quality of the soil and groundwater. The results obtained show that the native sulfur scattered in the environmental liability associated with the ancient sulfuric acid industry constitutes a potential source of sulfated acid drainage that locally affects the soil, groundwater, and underground structures of the industrial center, and also small adjacent ecosystems. The interaction between native sulfur and the rainwater causes the oxidation of the native sulfur releasing protons and sulfates, which reach the groundwater through the infiltration water process, generating the acidification of the environment. The results provide useful draft for the management of environmental liabilities, and also the monitoring data obtained could assist in prioritization of remediation options, which constitute a problem of relevance and whose regulations for management and mitigation are still a controversial issue.

Keywords Industrial waste · Native sulfur · Incubation tests · Oxidation tests · Sulfuric acid industry · Río de la Plata estuary

G. Albiero
Universidad Nacional de La Plata (UNLP), La Plata, Buenos Aires, Argentina

L. Santucci (✉) · E. Carol
Centro de Investigaciones Geológicas (CIG), Consejo Nacional de Investigaciones Científicas y Técnicas (CONICET), Universidad Nacional de La Plata (UNLP), Calle 64 y Diag. 113, 1900, La Plata, Buenos Aires, Argentina
e-mail: luciasantucci@fcnym.unlp.edu.ar

1 Introduction

Environmental liabilities are currently one of the most significant problems that affects the quality of both soils and groundwater and surface bodies. The closure of industries and the abandonment of environmental liabilities in their vicinities, added to urban growth in these areas, constitute a serious environmental concern. Highly contaminated soils are considered hazardous wastes that are highly harmful to the environmental system and human health (De Sousa, 2001; García et al., 2004).

Sulfated acid drainage constitutes an environmental problem which is frequently studied in mining waste derived from the exploitation of sulfides (Costa et al., 2008; Costa & Duarte, 2005; Delgado et al., 2019; Devasahayam, 2006; Idaszkin et al., 2017; Jennings et al., 2000; Lecomte et al., 2017; Lin, 1997; Ludwig et al., 2001; Nieto et al., 2013; Nieva et al., 2016, 2018; Nordstrom, 1982; Pons, 1973). In this type of

environmental liabilities, sulfides are oxidized to sulfates generating an acid drainage that affects the soil and release large amounts of sulfates and heavy metals into the water (Bigham & Nordstrom, 2000; Ferreira et al., 2020; Konner, 1993; Lin, 1997; Lin & Quvarfort, 1996; Lövgren et al., 1990; Schwertmann & Fitzpatrick, 1993; Turner & Kramer, 1992; Yang et al., 2009). Industries that use sulfur compounds as inputs in production processes (e.g., sulfuric acid production, agriculture, tire or rubber production, animal feed or pyrotechnics, pigment production, steel treatment, batteries production, and insecticides, bleaching paper) can also generate contamination during their storage, as well as generate waste through the discarded material (Tugrul et al., 2003). The scale of the issue and the quantity of sulfated acid drainage sites throughout the globe are factors that make sulfated acid drainage a critical environmental threat (Rezaie & Anderson, 2020).

On the other hand, the strategic position of coastal plains as a port route has led to the settlement of numerous industries. This leads to hydrological and ecosystem modifications given by setting up industries and urbanizations, which has entailed a considerable decrease of these coastal sectors worldwide (Carol et al., 2019; Costanza et al., 1993; Gerritse et al., 1990; Meire et al., 2005). The coastal plain of the Río de la Plata estuary develops on the northeast and east coast of the province of Buenos Aires, Argentina (Fig. 1). The coastal plain of the middle sector of the estuary between Berisso and Ensenada cities presents sectors with industrial activities associated with the development of a petrochemical center, where one of the biggest ports and refineries of Argentina was emplaced since the early 1920s (Fig. 1). The construction of the port and the industrial center required the filling and dug of canals of the naturally waterlogged area of the coastal plain, and such modifications caused strong changes in the hydrological behavior of this sector of the coastal plain (Santucci, 2020).

In Argentina, environmental liabilities constitute an environmental concern in many industrialized areas, mainly due to the scarce legislation that operated throughout the country before the 1990s. Among all industrial chemicals, sulfuric acid has large-scale uses within the chemical industry (Campbell et al., 1993; Müller, 1994). During the 1950s, Military Manufacturing Sulfuric Acid industry has been settled up in the vicinity of the petrochemical center, as consequence of industrial activity expansion (Fig. 1). Industrial waste has been mostly deposited in a sector adjacent to the ancient sulfuric acid industry nearby the Este Canal which is one of the canals surrounding the industrial site. Throughout the 1970s, the sulfuric acid industry finally closed and the waste was left on the industrial sector soil, leaving a polluted brownfield site. The residues, in which native sulfur dominate, are exposed to the air and are susceptible to alteration. Previous studies have shown that this environmental liability affects locally the quality of groundwater, with high concentrations of sulfates being registered in this sector of the petrochemical center, both in the unconfined and underlying semi-confined aquifers (Santucci, 2020; Santucci et al., 2017, 2018). The purpose of this work is to evaluate, from laboratory tests, the generation of sulfate acid drainage in environmental liabilities associated with the ancient sulfuric acid industry in order to identify the waste spatial distribution and to determine the impacts that they impart on the quality of the soil and groundwater. Identifying the area affected by the acid drainage generated by the waste and defining whether the groundwater is affected due to infiltration of soluble compounds such as sulfates through rainwater is essential when defining remediation and/or mitigation guidelines. Although in the studied area the groundwater is saline and is not used for human supply (Logan et al., 1999; Santucci et al., 2016), the soil and water of the ecosystems of the canal adjacent to the environmental liability may be affected by acid drainage. Likewise, the infrastructures of the petrochemical center may be deteriorated, generating greater environmental impacts (for example, deterioration of fuel storage tanks).

2 Study Area

The study area is located in the right margin of the middle Río de la Plata estuary within a sector between the cities of Ensenada and Berisso (Fig. 1a). Within this sector, the petrochemical center comprises a perpendicular strip along the coastline of approximately 1 km wide which is limited by three canals (Conclusión, Este, and Oeste) and by La Plata Port, located in the north (Fig. 1b). In the margin of Este Canal bordering the petrochemical center, environmental liabilities from an ancient sulfuric acid industry are present, covering a surface area of approximately 30,000 m2 (area indicated in red square in Fig. 1b). The study area was elevated nearly 2 m above the natural level due to

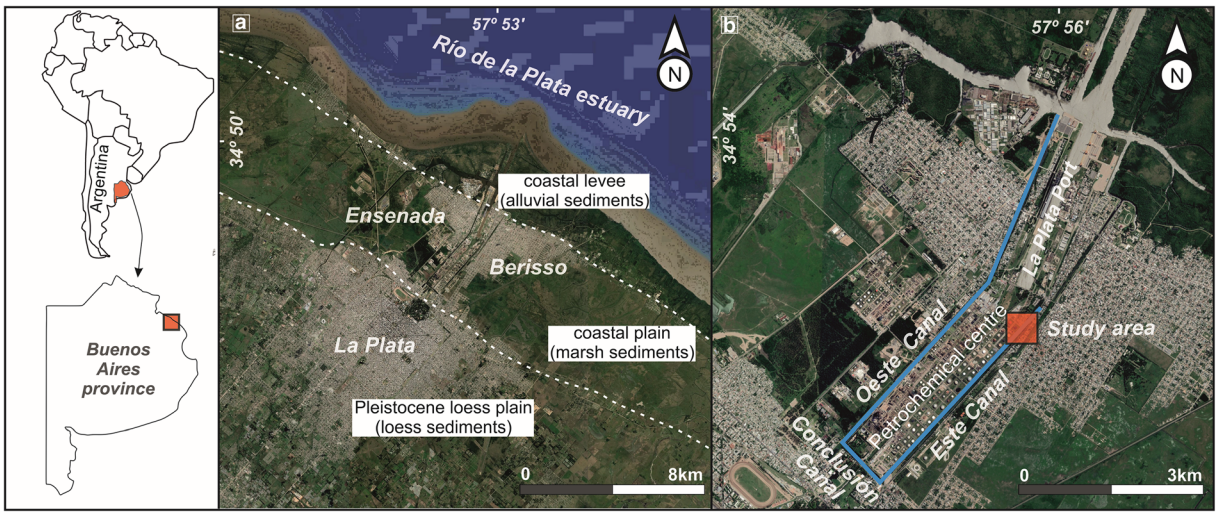

Fig. 1 **a** Location of the study area. **b** Environmental liability from the ancient sulfuric acid industry area is indicated in the red square

constant flooding, being the filling made with loessic sediments during the construction of the petrochemical center.

The study area is developed on the coastal plain of the Río de la Plata which is bounded by the Río de la Plata estuary in the East and by the Pleistocene loess plain in the West (Schnack et al., 2005; Fig. 1a). Within this sector, the Pleistocene loess, and Holocene marsh and alluvial sediments, host the unconfined aquifer. In the coastal plain, the Holocene sediments, of an average thickness of 6 m, are constituted by silt and clay that alternate with lenses of fine-grained sands and marine shells deposited over the loess sediments. The Pleistocene loess is composed of silt and sandy silt of eolian origin, with plagioclase, volcanic glass, and calcareous carbonates as the main components, showing an average thickness of 31.5 m (Carol et al., 2012). The Pleistocene loess is underlain by a Plio-Pleistocene sandy fluvial sediments, of a thickness between 12 and 30 m. The latter constitutes a highly productive of low salinity semi-confined aquifer in the most continental area. Between Pleistocene loess and Plio-Pleistocene sandy fluvial sediments, there is a silty-clayey layer with an average thickness of 3 m, which hinders the hydraulic transmission between the unconfined and the semi-confined aquifers. The uppermost coastal sediments consist of fine-grained sands that correspond to alluvial deposits of the levee located in the vicinity of the Río de la Plata (Fig. 1a). Based on the hydraulic head depths records, the regional groundwater flow is towards the Río de la Plata, while the local groundwater flow is towards the canals that were dug in the vicinity of the petrochemical center sector (Santucci et al., 2017). The hydraulic gradients are low, ranging from 0.0016 in the loess plain to 0.0006 or less in the coastal plain (Logan et al., 1999). In addition to receiving the contribution of continental water from groundwater discharge and surface runoff from the adjacent area, the canals receive tidal water from the Río de la Plata during the high tides events (heights above 2.5 m a.s.l), where the water can enters along the canals. This tidal influence may cause electrical conductivity variations in the water of the canal (Santucci, 2020).

3 Materials and Methods

Field surveys and sampling of the affected sediments from the ancient sulfuric acid industry located in the vicinity of the petrochemical center were carried out during May 2019, in order to identify the waste spatial distribution and to analyze the quality of the sediments. In addition, surface water from de Este Canal and groundwater from boreholes drilled to the unconfined aquifer were sampled during the same campaign.

3.1 Location and Survey of Sediment Samples

Based on the deposition of the environmental liability in the ancient sulfuric acid industry surroundings, the industrial waste area was identified, and sediment samplings were carried out in that sector. For the sediment

sampling, a sector adjacent to the Este Canal was defined, covering the entire area affected by industrial waste deposits, as well as the adjacent areas without waste deposits (Fig. 2a).

For sediment sampling, a grid was defined through four transects parallel to the Este Canal (Fig. 2b), which includes both sediment obtained from the environmental liability itself and from the canal bed. The grid has a total of 19 sampling points (Fig. 2b), and samples were taken from two depths (0–10 cm and 50–60 cm). An exception is constituted by the sediments obtained in the canal bed, since in this case only one sample of the bed was extracted per point. Samples 8 and 16 correspond to those sediments from the sector adjacent to the petrochemical center and are the samples farthest located from the Este Canal, while samples 3, 4, 7, 11, 15, and 19 were obtained from the bed of the canal. The rest of the samples, located within the red polygon in the center of the grid, correspond to those within the environmental liability itself.

Sediment samples from the sector with the scattered deposits were collected using a gouge auger, removing the outer layer of each core and discarding it to avoid contamination. To evaluate the drag of these residues towards the Este Canal, sediment surface samples were taken directly from the bed of the canal. All samples were placed into thick plastic bags and refrigerated transported to the laboratory for analyses.

3.2 Sediments Mineralogy

The mineralogical composition in some selected samples was determined by X-ray diffraction analysis (XRD) using a PANalytical brand X-ray diffractometry equipment, model X'Pert PRO with Cu lamp (kα = 1.5403 Å) that operates at 40 mA and 40 kV. Previously, samples were air-dried and ground with an agate mortar. The analysis of the total fraction was carried out in the range from 5 to 65° 2θ. The identification of the phases was carried out using the X'Pert High Score Plus v3.0e software from PANalytical. In addition, thin sections of waste samples were made for polarized microscopic examination (polarization microscope Nikon Eclipse E-200).

3.3 Laboratory Determinations on Sediment Samples

The sediments samples were oven dried at 40 °C and were milled with porcelain mortar. In each sample, a quartering was carried out, and subsequently incubation pH and oxidation pH were determined.

The incubation pH was determined according to the international standard NF ISO 10390 (1994) and Konsten et al. (1988), and it was carried out during 8 weeks in the whole sediments samples. Sediment pH was measured on 1:5 sediment:water suspensions, that means, 10 g of dry sediment sieved to 2 mm were taken and 50 mL of distilled water was added, then it was shaken for 1 h on an oscillating table, it was left to settle for 30 min, and the pH was finally measured by immersing the pH electrode. Electrical conductivity (EC) was also measured in 1:5 sediment:water suspensions using Lutron Model WA-2017SD multiparametric equipment.

The oxidation pH was determined according to Watling et al. (2004), in the whole sediment samples. During the procedure, 2 g of dry sediment sample were weighed and placed in glass beakers. After, a 30% hydrogen peroxide solution was applied in the form of eye drops and stirred with a glass rod. Prior to taking measurements, each sample was left 15 min for all reactions to take place and for them to cool down. Subsequently, the pH and EC of the paste was measured, for which a Lutron Model WA-2017SD multiparametric equipment was used. This laboratory test allowed the assessment of the maximum oxidation of the native sulfur residues contained in the sediment samples.

3.4 Water Monitoring Network and Water Sampling

In order to characterize the impact of the environmental liability left by the ancient sulfuric acid industry on the water, it was defined a monitoring network of shallow groundwater and surface water in the Este Canal. Groundwater samples were collected from exploration boreholes drilled on the margin of the Este Canal, while surface water samples were collected with bottles directly from the canal. The groundwater sampling network comprises 4 sampling boreholes reaching a depth of up to 6 m in the unconfined aquifer, comprising sectors within the environmental liability and others in its vicinity (Fig. 2a). The surface water samples were obtained at 3 points in the Este Canal, one point near the main waste sector, and two others, one upstream and the other downstream the canal. In all water samples, pH and electrical conductivity were measured in situ using a Lutron Model WA-2017SD multiparametric equipment.

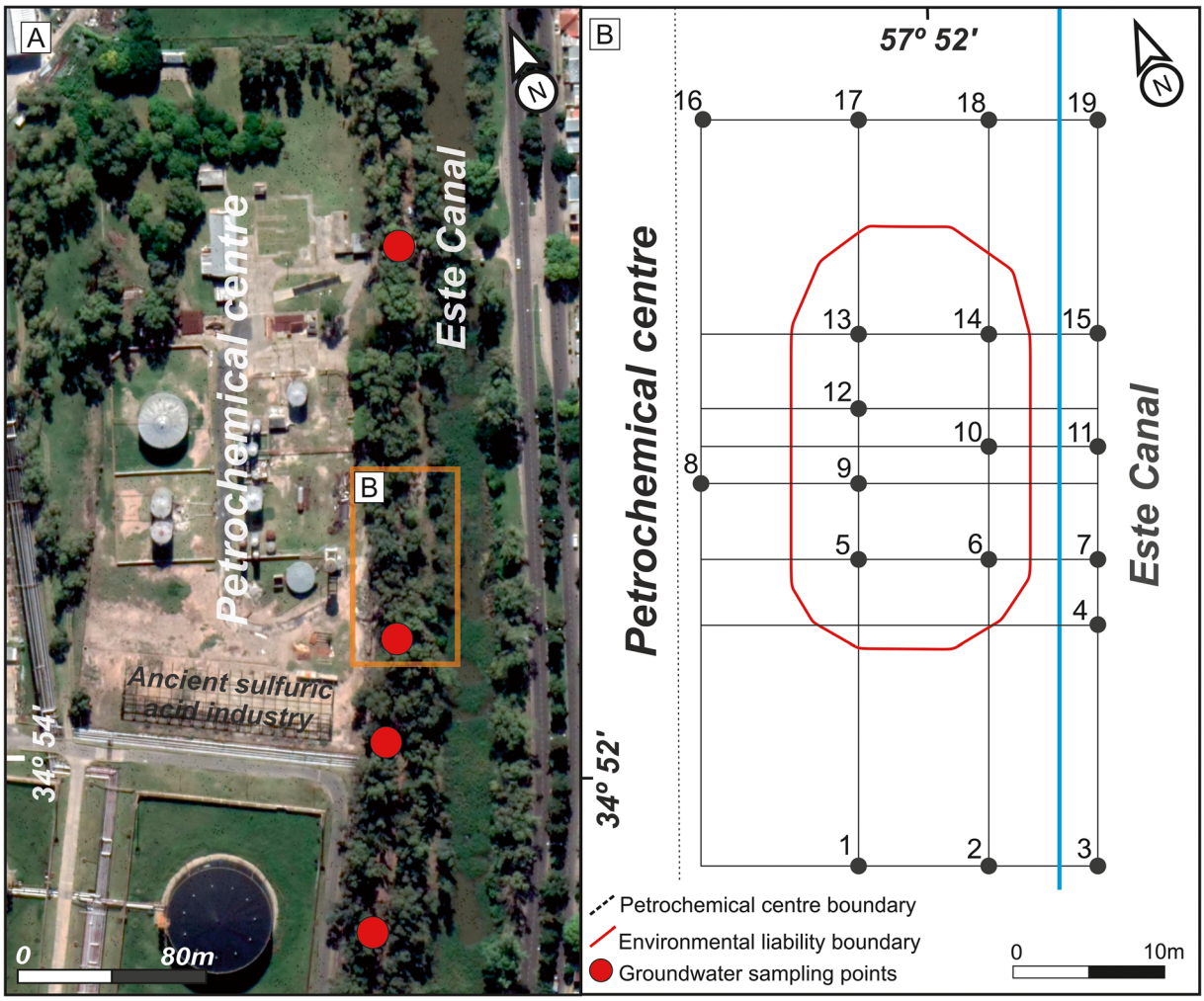

Fig. 2 **a** Detailed section of the study area and the sector where the sediment samples were taken (orange rectangle) and location of the groundwater sampling points. **b** Sediment sampling grid, represented in Fig. 2b in the orange rectangle

The water sampling was carried out according to standard methods (APHA, 2017), and the bottles were stored refrigerated until chemical determinations in the laboratory.

3.5 Laboratory Determinations on Water Samples and Aliquots from the Essays

In groundwater samples and those obtained from the Este Canal, the soluble sulfate content was determined in triplicate in order to evaluate the impact on the water resource, due to the sulfur oxidation coming from the industrial waste. In the sediment samples, where both the incubation pH and the oxidation pH were determined, the aliquot generated as a result of these techniques was extracted, on which the soluble sulfate content was also determined.

Soluble sulfate (SO_4^{2-}), in each 1:5 sediment:water extract from both the incubation and oxidation pH essays, was analyzed through turbidimetric method (APHA, 2017) using a Shimadzu UV - 160A Dual Beam Visible Spectrophotometer - 160A; sulfate in groundwater and surface water samples was also analyzed. The determination of sulfates in the incubation pH aliquots will allow the evaluation of the oxidation of the sulfur contained in the industrial residue resulting from the infiltration of rainwater, as well as the contributions of sulfates to the groundwater produced by that process. On the other hand, the determination of sulfates in the aliquot extracted from the oxidation pH test will

allow the evaluation of the maximum oxidation of the sulfur residues contained in the soil as well as the maximum contribution of sulfates to the groundwater derived from them. The entire analysis were performed in the Centro de Investigaciones Geológicas (CIG).

4 Results

4.1 Properties and Mineralogy of the Sediments

Within the environmental liability area and in the surrounding sector, abundant grains of native sulfur of sizes between 4 and 15 mm scattered on the soil surface are observed (Fig. 3a). Mineralogical determinations from XRD showed the presence of quartz, plagioclase, feldspar, anhydrite, jarosite, gypsum, native sulfur, and hematite in the analyzed sediments (Fig. 3b, c). Likewise, a release is observed in the background of some of the diffractograms (Fig. 3b) that would indicate the presence of amorphous minerals and/or organic matter. The observation of the sediment samples by means of the polarized microscope displays that the native sulfur grains are fractured showing an alteration zone both in the fractures areas and in the edges of the grains (Fig. 3d). In the most clastic deposits composed mainly of quartz-feldspar type silicates, the alteration of the native sulfur grains can be observed, as well as the arrangement of native sulfur in the finer matrix that surrounds the silicatic clasts (Fig. 3e).

4.2 Variation of pH, Electrical Conductivity, and SO_4^{2-} Release from Sediments During Incubation and Oxidation Tests

The spatial variation of the pH, electrical conductivity, and sulfate values was displayed by the confection of isoline maps which were made using QGIS 2.8.3 software (QGIS, 2020). Although the pH and electrical conductivity values were measured in the 8 weeks of the incubation test, these maps were made for the pH and EC values corresponding to weeks 1, 4, and 8, and also for the pH values obtained in the oxidation tests. The SO_4^{2-} data obtained were also plotted in maps for weeks 1, 4, and 8 of incubation test and for those obtained from the oxidation pH tests.

4.2.1 Incubation pH Tests

During the incubation pH tests carried out during 8 weeks in the sediments, an increase in pH was observed from the first week to the last one, both in the samples obtained between 0 and 10 cm in depth and in those extracted between 50 and 60 cm in depth (Table 1). The pH values recorded in the more surface sediments vary between 1.4 and 6.6 in week 1 (W1) and between 2.5 and 6.6 in the fourth week (W4), while for week 8 (W8), the minimum and maximum values were 3.0 and 6.8 respectively. On the other hand, in 50—60-cm depth, the pH values vary between 1.8 and 4.5 in the first week (W1), between 2.8 and 4.8 for the fourth (W4), and between 3.3 and 5.0 for the last one (W8).

From the analysis of the spatial distribution of the samples, it is observed that the lowest pH values for each week are recorded at the same sampling point at both depths and correspond to the point located particularly on the environmental liability corresponding to sample 12 (see grid in Fig. 2b, e, g; Fig. 4a, b). On the other hand, the less acid values are represented in the margins of the maps, both in surface and in depth samples. When examining the isolines pH maps, it is evident that towards the Este Canal, there is a displacement of the lower pH values where higher values take place (Fig. 4a–f).

4.2.2 Oxidation pH Tests

The pH values obtained in the surface sediment samples exposed to hydrogen peroxide solution range from 1.3 to 5.9 (Fig. 4g), while for those of greater depth range from 1.6 to 4.5 (Fig. 4h). It is worth noting that as in incubation pH tests, the most acid values are found in the center of the study area where the accumulation of residues is greater. Likewise, higher values of pH take place towards the Este Canal (Table 1; Fig. 4g, h).

4.2.3 Electrical Conductivity Variations

The electrical conductivity data obtained from surface sediment samples ranged between a minimum of 130 and a maximum of 5374 μS/cm for the first week (W1), 49 and 3280 μS/cm for week 4 (W4), and between 19 and 1821 μS/cm for week 8 (W8). The deeper sediment samples obtained showed values between 236 and 8430 μS/cm for the first week (W1), between 70 and 2210

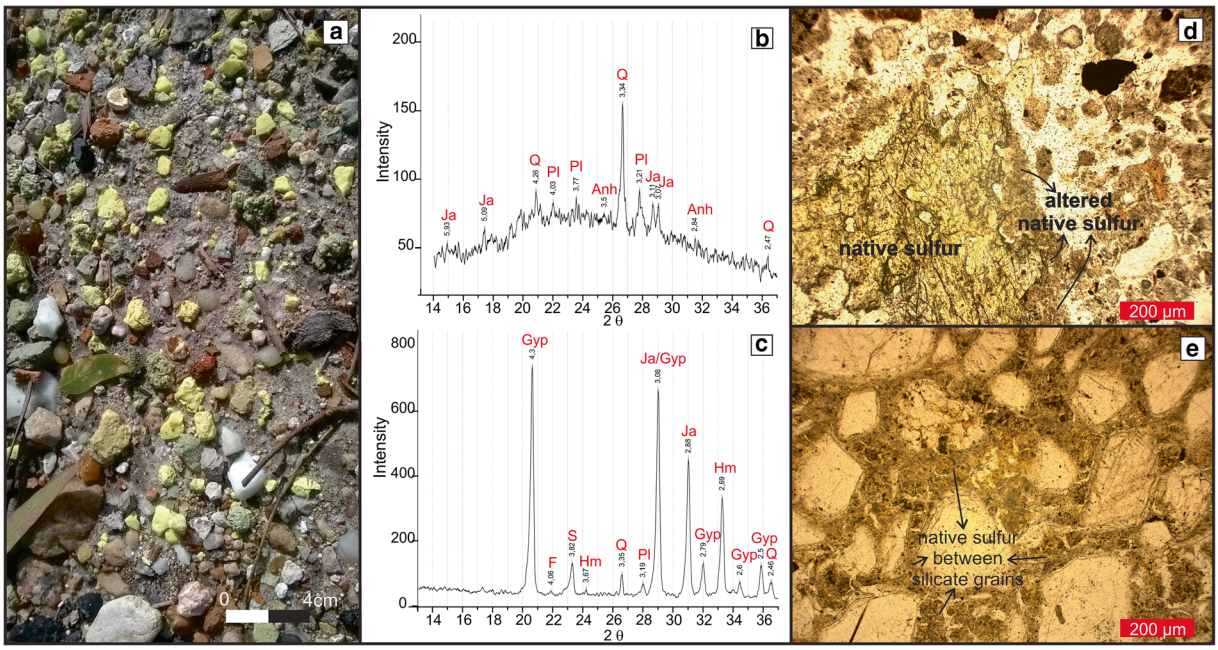

Fig. 3 **a** Grains of native sulfur and sediment remains from fill and construction in the sector affected by wastes of the ancient sulfuric acid industry. **b**, **c** X-ray diffractograms of sediments. Q, quartz; Pl, plagioclase; F, feldspar; Anh, anhydrite; Ja, jarosite; Gyp, gypsum; S, sulfur; Hm, hematite. **d**, **e** Thin section photographs showing the altered native sulfur grains and those grains of sulfur scattered between grains of silicates

µS/cm for week 4 (W4), and between 22 and 1509 µS/cm for last week (W8) (Table 1).

During the first week (W1) in which the tests were carried out, the highest values of electrical conductivity were observed, both at a superficial and deeper level and these correspond to the samples taken from the sector where the environmental liability is spread (Fig. 5a, b). In particular, for the deeper sediment samples, an electrical conductivity increase is observed towards the sector of the upper right margin of the grid (Fig. 5b). During week 4 (W4), it can be observed, through the isoline maps of electrical conductivity, that the values clearly decrease, but the highest values are still focused on both the surface and deeper sediment samples located in the sector where the environmental liability is scattered (Fig. 5c, d). Finally, for week 8 (W8), the electrical conductivity values decrease for both the superficial and deeper sediment samples to the lowest values recorded during the tests (Fig. 5e, f).

4.2.4 SO_4^{2-} Release from Sediments with Native Sulfur

The sulfate contents obtained in the aliquots from the pH incubation tests of surface sediment samples ranged between 34 and 2936 mg/L in week 1 (W1), between 7 and 334 mg/L at week 4 (W4), and 9 and 358 mg/L at week 8 (W8; Table 1). The sediment samples obtained deeper showed values between 41 and 2044 mg/L, between 2 and 313 mg/L, and 18 and 188 mg/L of sulfates for the first, fourth and eighth weeks (W1, W4, and W8) respectively (Table 1).

Sulfate concentrations decrease as the weeks progress in time, as can be seen in Fig. 6. The highest sulfate values during week 1 (W1) are concentrated in the central sector of the sampling grid corresponding to samples 9 and 12 (see grid in Fig. 2b), both on the surface and in depth (Fig. 6a, b). In contrast to week 1, where the highest values of sulfates were around 2000 mg/L in the central area of the grid, during week 4 (W4), there is an evident decrease in the sulfate concentration at both depths with values that do not exceed 400 mg/L (Fig. 6c, d). This trend is also seen in the eighth week (W8) with a decrease in the sulfate concentration, although more attenuated, with maximum values near 100 mg/L (Fig. 6e, f).

The sulfate data obtained in the samples to which hydrogen peroxide was added in the oxidation tests show concentrations between 82 and 2000 mg/L in the

Table 1 Values of pH, electrical conductivity (EC), and sulfate concentration in the extracts from the incubation tests for weeks 1, 4, and 8, and oxidation tests. The location of the samples is indicated in the grid of Fig. 2b

Sample	Depth/type	Oxidation test		Incubation test (week 1)			Incubation test (week 4)			Incubation test (week 8)		
		pH	SO_4^{2-} (mg/L)	pH	EC (μS/cm)	SO_4^{2-} (mg/L)	pH	EC (μS/cm)	SO_4^{2-} (mg/L)	pH	EC (μS/cm)	SO_4^{2-} (mg/L)
1	0–10	4.1	812	4.9	130	95	4.7	69	7	4.7	38	35
1	50–60	3.7	494	4.0	236	40	4.2	115	2	4.5	34	67
2	0–10	2.3	170	3.4	226	129	3.6	165	13	3.7	111	47
2	50–60	2.8	1021	3.6	498	122	4.1	125	17	4.4	43	45
3	Canal	4.0	844	5.2	430	54	5.7	111	17	5.8	71	41
4	Canal	3.1	1716	3.7	3982	408	4.0	617	17	3.9	445	18
5	0–10	2.6	490	2.7	3598	933	3.2	1901	34	3.5	1059	173
5	50–60	2.5	1423	2.9	3598	912	3.4	2120	40	3.5	939	93
6	0–10	2.6	335	3.0	278	265	3.5	179	44	3.7	95	21
6	50–60	2.3	1062	2.7	986	306	3.1	420	85	3.3	214	18
7	Canal	3.9	1335	4.6	776	367	4.8	512	112	4.7	294	357
8	0–10	3.8	388	4.3	334	204	4.5	77	7	5.1	19	65
8	50–60	4.5	381	4.5	1186	490	4.8	560	17	5.0	331	47
9	0–10	2.5	531	2.5	5374	1096	3.1	2260	333	3.3	1512	190
9	50–60	2.6	1226	3.0	8430	1635	3.4	1443	194	3.4	1091	132
10	0–10	4.0	426	5.6	324	47	6.6	193	17	6.8	1346	41
10	50–60	2.2	367	3.5	442	231	4.1	179	17	4.5	88	19
11	Canal	2.6	1478	3.9	794	688	4.1	541	19	4.0	278	44
12	0–10	1.3	1257	1.4	4918	2936	2.5	3280	299	3.0	1821	188
12	50–60	1.6	1873	1.8	5425	2043	2.8	2210	231	3.3	1509	188
13	0–10	2.5	463	2.7	2714	340	3.3	1473	29	3.5	578	91
13	50–60	2.6	694	3.0	2566	299	3.4	1335	65	3.5	1364	167
14	0–10	2.7	613	3.1	360	122	3.5	159	36	3.8	75	9
14	50–60	2.1	430	2.4	3598	286	2.9	642	48	3.4	156	58
15	Canal	4.8	957	6.0	498	81	6.4	293	34	5.9	223	16
16	0–10	3.5	2084	4.0	438	136	4.5	113	27	4.7	37	65
16	50–60	3.6	245	4.1	278	68	4.7	70	74	5.0	22.0	46
17	0–10	3.3	1062	3.7	518	143	4.2	196	53	4.5	43	72
17	50–60	3.4	531	3.7	2510	381	4.0	1422	51	3.9	1207	144
18	0–10	3.3	2000	4.2	148	218	4.7	49	20	4.6	37	89
18	50–60	2.9	245	3.3	3158	224	3.6	1127	313	3.8	330	37
19	Canal	5.9	81	6.6	354	34	6.3	356	10	6.6	136	12

surface samples and between 245 and 1873 mg/L in the samples obtained at depth (Table 1). At 50–60 cm deep, the highest concentrations of sulfate were recorded in the central zone of the sampling grid (values between 1200 and 1800 mg/L), coinciding with the sector with the highest occurrence of the scattered sulfur fragments (Fig. 6h).

4.2.5 Relations Between pH, Electrical Conductivity, and SO_4^{2-}

Comparing pH and electrical conductivity values obtained in the sediment samples from week 1 to 8 of the incubation test, it is observed that the pH values decrease as the electrical conductivity increases in both the

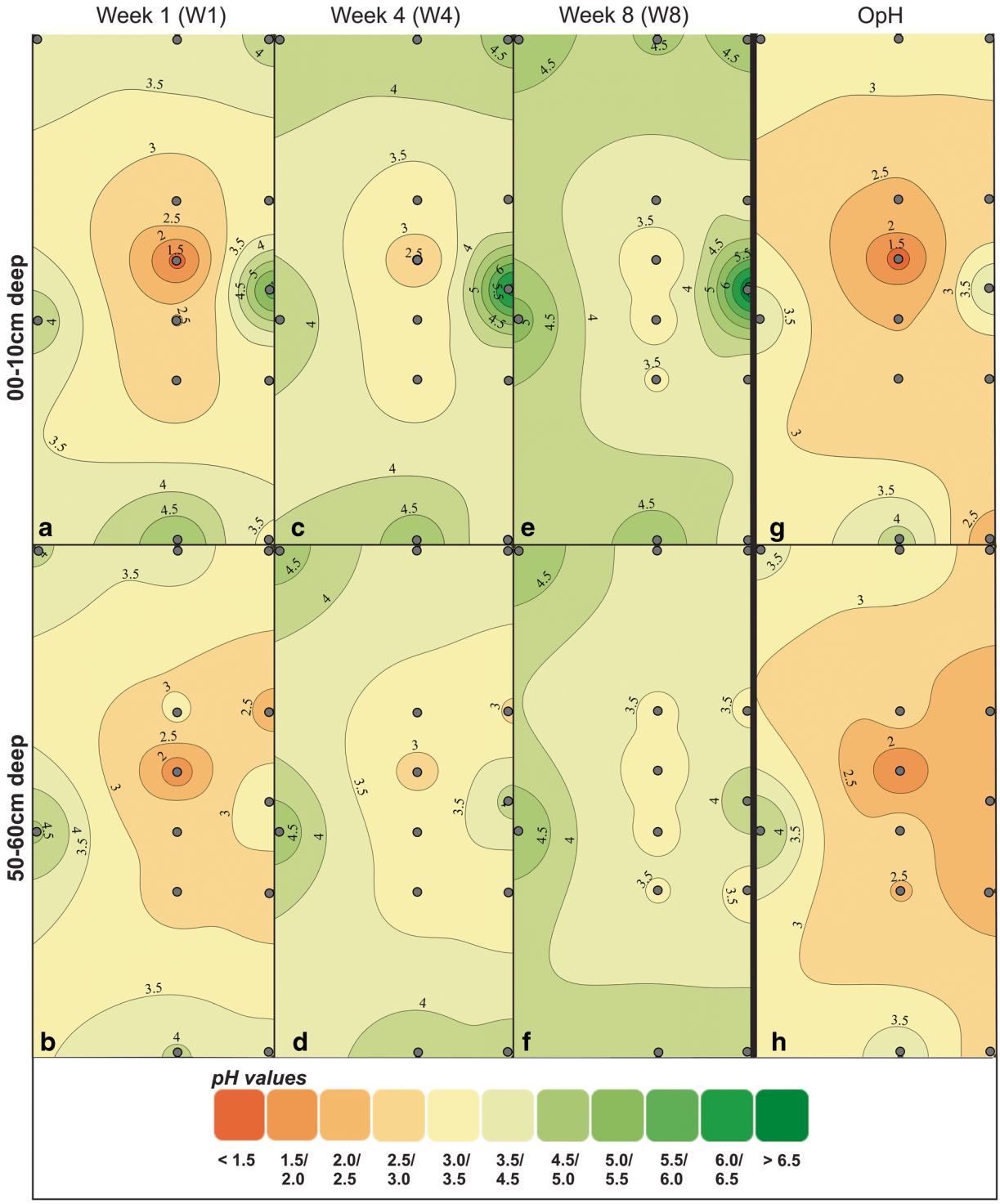

Fig. 4 Isoline maps, determined by using QGIS 2.8.3 software, of pH values obtained for the sediments analyzed in the sector, both superficial (0–10 cm deep) and in deep (50–60 cm deep), and for weeks 1, 4, and 8 of incubation pH test (W1, W4, and W8) and for the oxidation pH test (indicated as OpH)

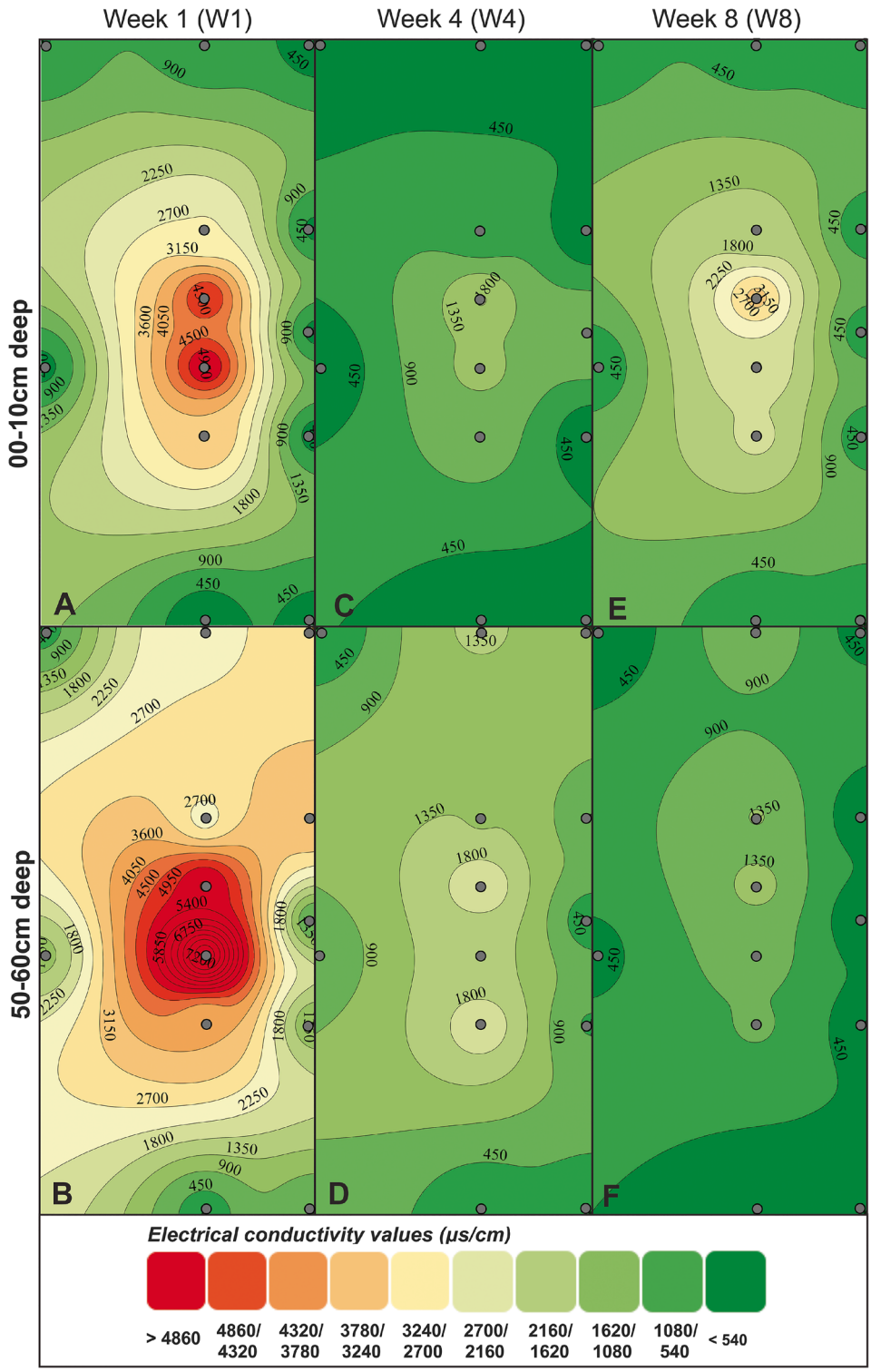

Fig. 5 Isoline maps, determined by using QGIS 2.8.3 software, of electrical conductivity (EC) values (µS/cm) obtained for the sediments analyzed in the sector, both superficial (0–10 cm deep) and in deep (50–60 cm deep), and for weeks 1, 4, and 8 of incubation pH test (W1, W4, and W8)

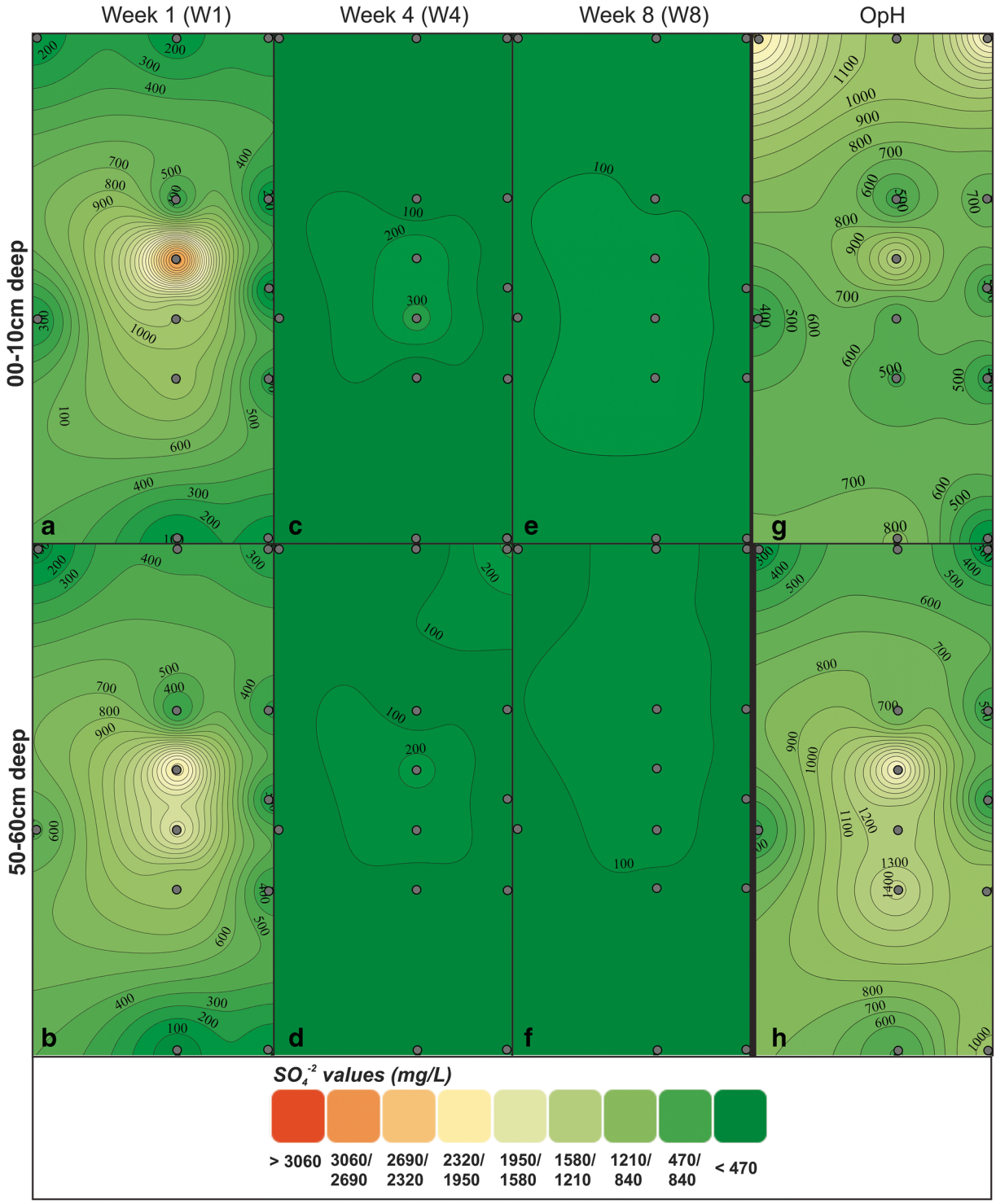

Fig. 6 Isoline maps, determined by using QGIS 2.8.3 software, of sulfate values (mg/L) obtained for the sediments analyzed in the sector, both superficial (0–10 cm deep) and in deep (50–60 cm deep), and for weeks 1, 4, and 8 of incubation pH test (W1, W4, and W8) and for the oxidation pH test (indicated as OpH)

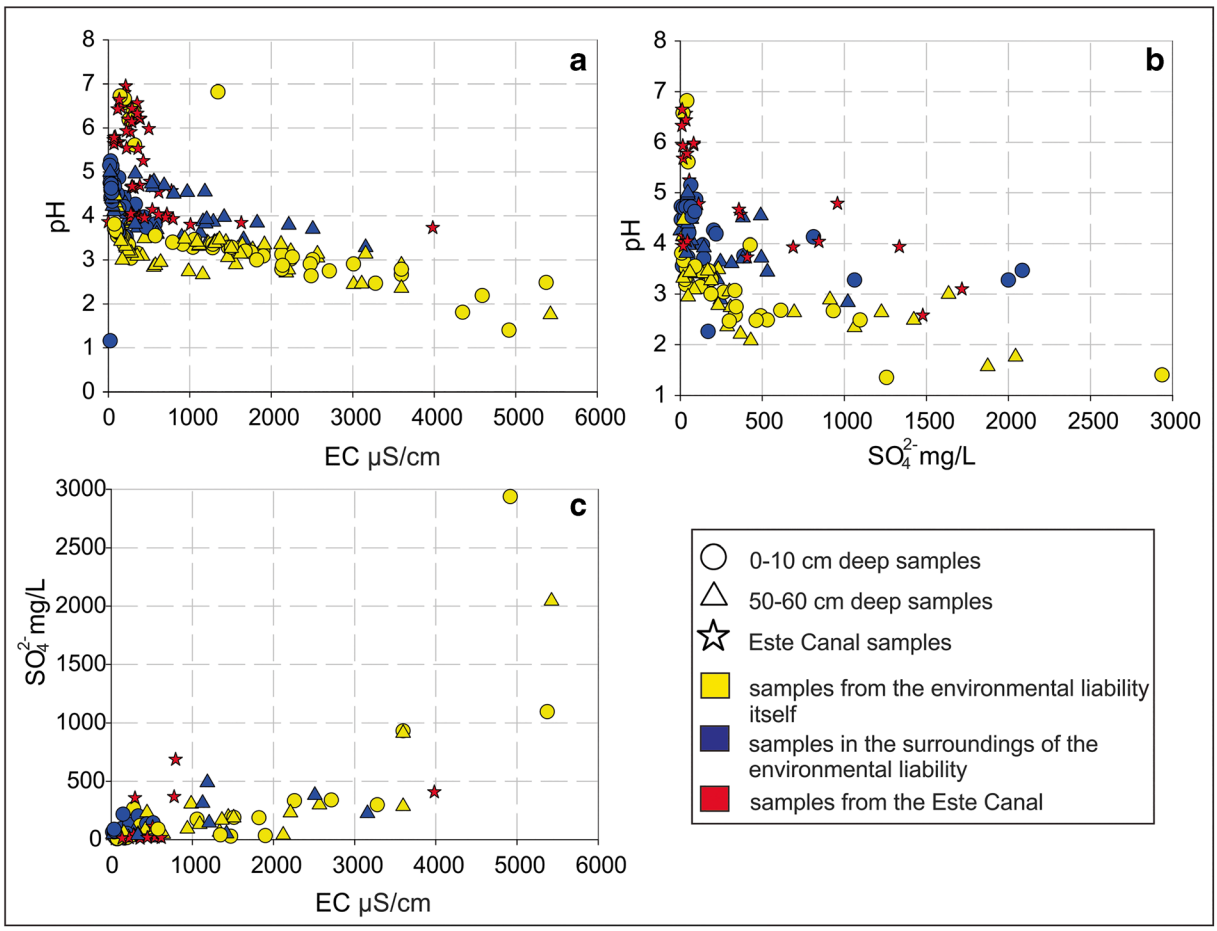

Fig. 7 Relations of **a** pH vs. electrical conductivity for the 8 weeks of the incubation test. **b** pH vs. sulfates for weeks 1, 4, and 8 of the incubation test. **c** Sulfates vs. electrical conductivity for weeks 1, 4, and 8 of the incubation test. Yellow samples correspond to those located in the center of the grid in the environmental liability itself (inside the red polygon in Fig. 2b). Blue samples correspond to those located in the surroundings of the environmental liability (outside the red polygon, see Fig. 2b)

most superficial samples (circles) as in those obtained at 50–60 cm deep (triangles; Fig. 7a). It should be noted that the samples located in the environmental liability itself show the lowest pH values and the highest in general correspond to the samples obtained from the Este Canal.

Table 2 Values of pH, electrical conductivity, and SO_4^{2-} concentration in surface and groundwater samples

Type of sample	pH	CE (µS/cm)	SO_4^{2-} (mg/L)
Surface water	7.50	853	20.44
	7.40	675	13.63
	7.38	900	25.89
Groundwater	5.82	5610	1008.32
	7.24	11510	1819.06
	4.26	6440	735.80
	6.84	11590	1301.28

In the graph pH vs. SO_4^{2-} it is observed that the pH values in the sediment samples decrease as the SO_4^{2-} values increase, both in the more superficial samples and in those obtained at 50–6 0cm deep, and particularly in the samples located in the environmental liability itself (Fig. 7b). It is worth noting that the highest sulfate values and the lowest pH values are observed during the oxidation test and for week 1 of the incubation test (Table 1).

On the other hand, in the graph of Fig. 7c, it can be observed that the higher the SO_4^{2-} values obtained in the incubation tests correspond to the higher the electrical conductivity values. As mentioned above, the highest

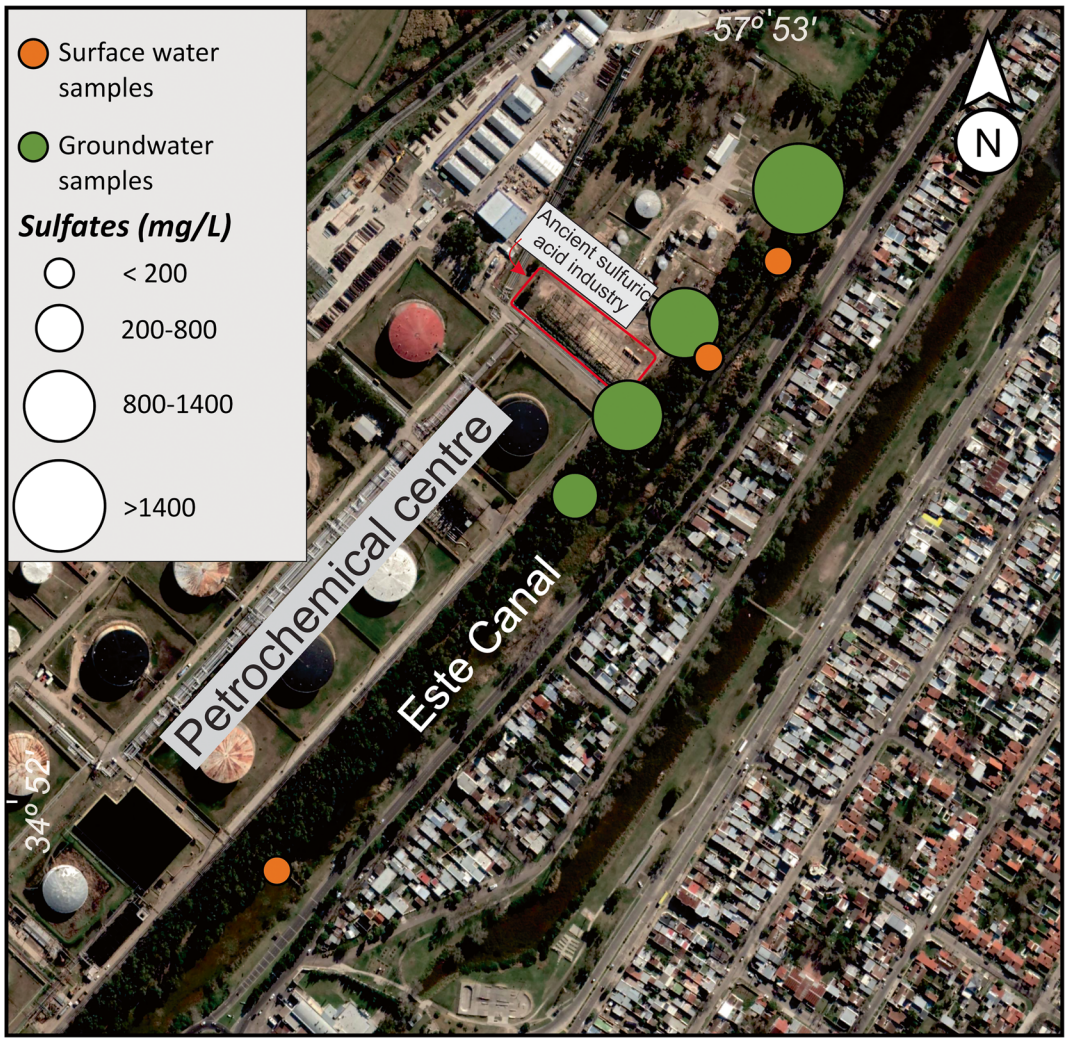

Fig. 8 Water sampling network in the vicinity of the petrochemical center area and sulfate contents in surface and groundwater samples

values of sulfate and electrical conductivity are observed in week 1 of the incubation test carried out, both in superficial and 50–60 cm deep samples. In addition, the lowest EC values correspond to the samples obtained from the Este Canal.

4.3 pH, Electrical Conductivity, and Sulfate Content in Groundwater and Surface Water in the Vicinity of Environmental Liabilities

The pH in the surface water samples shows values between 7.38 and 7.50, while pH in groundwater samples varies between 4.26 and 7.24 (Table 2). The electrical conductivity data show values between 675 and 900 μS/cm for the surface water samples, while the groundwater samples present values between 5610 and 11590 μS/cm (Table 2).

The chemical composition of water regarding sulfate concentration registers variations in both the groundwater and surface water samples from the Este Canal in different sectors of the study area adjacent to the ancient sulfuric acid industry (Table 2; Fig. 8). Groundwater shows sulfate contents between 735.80 and 1819.06 mg/L, being the highest values registered towards the northeast sector of the environmental liability (Fig. 8; Table 2) and the lowest towards the southwest (Fig. 8; Table 2). On the other hand, in the surface water samples obtained from the Este Canal, the sulfate content varies between 13.63 and 25.44 mg/L (Fig. 8; Table 2), showing that sulfate concentrations do not show significant variations along the Este Canal.

5 Discussion

This study examines sulfur mineral oxidation in acid sulfate soil materials during incubation and oxidation methods in a sector where waste deposits from an ancient sulfuric acid industry are located. The results obtained in the laboratory tests carried out on the sediments of the environmental liability show that the industrial waste constitutes a potential source for the development of acid drainage in the sediments that also affects the groundwater and surface water bodies in the surroundings of the environmental liability. The incubation method has been used to simulate the oxidation of acid sulfate soil materials under natural conditions to observe the behavior of these materials during oxidation (e.g., Crockford & Willett, 1995; Dent, 1986; Ward et al., 2004a,b). Although the conventional incubation method simulates oxidation under field conditions, a potential disadvantage of this method is that oxidation products build up within the incubated soil; whereas in the natural environment, they are subject to removal by leaching (van Breemen, 1973). That is why in the tests carried out for this work, the oxidation products were extracted every week from the incubated sediment, leading to a proper representation of leaching that would occur in natural environments. Thus, incubation tests show how the interaction of water with the sediments of the environmental liability causes an acidification of the sediments, which reach pH values lower than 2 in the central sector of the environmental liability. For this tests, the water from the extract obtained represents the water that, after interacting with the sediments, can infiltrate into the groundwater unconfined aquifer. Regarding this, note that the decrease in the pH of the sediments is accompanied by an increase in the electrical conductivity and sulfate contents in the extract water (Fig. 7a, b), which are high the first week and then, as a consequence of washing, their values tend to decrease. This shows that the environmental liability would affect the groundwater causing an increase in the concentration of sulfates which would also lead to an increase in the electrical conductivity of the groundwater (Fig. 7c; Fig. 8). Likewise, this interaction of water with sediments affects the Este Canal water quality, to which the sulfates enter from the environmental liability sector either by surface runoff or groundwater discharge.

On the other hand, the results obtained in the oxidation pH tests would be indicating the maximum acidity that the sediments can reach, as well as the highest amount of sulfates that can be released into the aquifer. In these tests, the acidification is greater with pH values lower than 3 being recorded in most samples. Regarding the release of sulfates, it is important to point out that the redox processes take on an important relevance, since the sulfates released in this case would be associated mostly with the oxidation of native sulfur. This does not rule out that there may be other sources of sulfates (e.g., gypsum) that can be released in addition to native sulfur during the incubation tests.

The study of mineral phases, which are present in the sediments, and the water sulfate contents make it possible to interpret the geochemical processes taking place in the topsoil. In this sense, jarosite was identified in XRD, whose presence indicates acidic pH conditions that currently affect the soil (Santucci et al., 2018). The determination of pH, electrical conductivity, and content of sulfates carried out in groundwater from shallow exploration wells located in the vicinity of the environmental liability allows to show the impact that this currently produces on the groundwater resource. Note that the groundwater samples located in the environmental liability sector and downstream of it reach sulfate values higher than 1400 mg/L, while upstream and in the refinery zone, these values are lower than 200 mg/L (Ainchil and Kruse, 2002; Logan et al., 1999; Santucci et al., 2018). In this sense, it is worth to highlight that the spatial extension of the high sulfate content, and consequently the electrical conductivity and pH values, is rather limited due to the low hydraulic gradient in the coastal plain (in the order of 10^{-4}), which determines that the groundwater flow will be extremely slow (Logan et al., 1999). Thus, the values recorded in the water evidence a prolonged affection over time, which, given the slow groundwater flow, would further increase the problem in the future. On the other hand, the sulfate contents in the Este Canal are low and this can be explained by the periodic inlet of the tidal water into the canal that could produce its washing and water renewal.

In relation to the processes that involve the generation of acid drainage and the release of sulfates, these would occur mainly in the unsaturated zone where oxidizing conditions dominate. Within the unsaturated zone, the rainwater that infiltrates the sediments of the environmental liability comes into contact with the native sulfur fragments. The native sulfur is oxidized (Hemireaction 1), while the $O_{2(g)}$ dissolved in the water is reduced (Hemireaction 2), releasing SO_4^{2-} and H^+

ions into the water in these reactions (Eq. 1), and causing the environment acidification.

$2*[S° + 4H_2O \longrightarrow 8H^+ + SO_4^{2-} + 6e^-]$ E°= − 0.65 mV (Hemireaction 1)

$3*[O_2 + 4H^+ + 4e^- \longrightarrow 2H_2O]$ E°= 1.23 mV (Hemireaction 2)

$$2S^{\circ} + 2H_2O + 3O_2 \longrightarrow 4H^+ + 2SO_4^{2-} \quad (1)$$

The set of these reactions explains the generation of acid drainage and the contribution of sulfates to the groundwater with the infiltration of rainwater. However, it is not ruled out that there may be other redox reactions involved in these processes that affect the pH of the soil and the quality of the groundwater in the vicinity of the industrial sector. Also the presence of sulfur-oxidizing bacteria play important roles in redox reactions (Diao et al., 2018). Sulfur-oxidizing bacteria can be colorless sulfur bacteria, which oxidizes reduced sulfur compounds using oxygen or nitrate as electron acceptor (Sweerts et al., 1990). Other groups of bacteria include green sulfur bacteria and purple sulfur bacteria, which can use sulfide, elemental sulfur, and thiosulfate as electron donors in anoxygenic photosynthesis (Frigaard & Dahl, 2008).

The pH, EC, and SO_4^{2-} values obtained in the incubation tests show a strong impact on the soil and water in the first week and then these values decrease in weeks 4 and 8 due to the washing and extraction of the aliquot in each sample. This is because when grinding the sediments for the laboratory tests, the grain size is reduced and the exposure surface is increased, favoring oxidation and therefore the release of more SO_4^{2-} and H^+ ions into the water. However, in the environmental liability, the size of the sulfur grains was considerably larger (Fig. 3), thus reducing the surface of the mineral exposed to react. The presence of abundant grains of native sulfur of sizes between 4 and 15 mm determines that these grains will be altered more slowly over time.

Oxidation of reduced inorganic sulfur species and formation of actual acid sulfate soils has an enduring and complex effect on the soil and surrounding environment (Corfield, 2000). This also occurs with mining waste derived from the exploitation of sulfides where these are oxidized to sulfates generating an acid drainage that affects the soil and release large amounts of sulfates and heavy metals into the water (e.g., Costa & Duarte, 2005; Devasahayam, 2006; Ferreira et al., 2020; Jennings et al., 2000; Lin, 1997; Lin & Quvarfort, 1996; Nordstrom, 1982; Pons, 1973). The canals that surround the petrochemical center constitute small ecosystems within a strongly anthropized area. As mentioned above, the entrance of tidal water into the canals produces a renewal of the water that leads to maintaining its pH and diluting the sulfate contents; however, in the canal substrate. the sediments contain high sulfur concentrations. Although this element can act as nutrients for plants, high levels of bioavailable sulfur can be harmful to them (Rennenberg, 1984; Schmidt & Jäger, 1992). Nevertheless, given that the environmental liability is located in an industrial sector and that the area of affectation is very local, there would be no relevant impact on the ecosystems. It should be noted that natural wetland areas that develop in adjacent sectors within the coastal plain area are characterized by also presenting high levels of sulfates. In this cases, the presence of sulfated water is associated with the oxidation of sedimentary pyrite (Logan & Nicholson, 1998), unlike the area studied in this work where the contributions of sulfates derive from industrial waste (Santucci et al., 2018).

Likewise, although a negative impact on the quality of groundwater exists, it is not exploited for supply due to it has high saline contents within the study area of the coastal plain (Logan et al., 1999; Santucci et al., 2016). However, within the study area, the underground pipelines that connect the petrochemical center with the port may be affected by the acid drainage generated by environmental liabilities. The acidity generated from acid sulfate soils can result in the corrosion of concrete and steel infrastructure, which can cause significant financial losses (Ljung et al., 2009; Pradhan, 2014; Shaheen & Pradhan, 2017; Zhou et al., 2018), as well as a greater environmental impact in case, for example, a fuel pipeline breaks.

6 Conclusions

The results obtained allow us to conclude that the environmental liability associated with the ancient sulfuric acid industry that is located in a sector of the petrochemical center adjacent to the Este Canal, constitutes a source of sulfated acid drainage that locally affects the soil and groundwater.

The presence of significant amounts of native sulfur in the sediments that constitute the environmental liability is the main cause of generation of sulfated acid drainage. This environmental liability has been located in the area studied for about 50 years and is liable for the high concentrations of sulfates registered in the groundwater in its vicinity. Although the water is not used for human supply, the high concentrations of sulfates can corrode the underground structures of the industrial center. On the other hand, the water and ecosystems developed in the Este Canal are affected but to a lesser extent since the periodic entry of the tidal water allows the renewal and washing of the canal water.

The laboratory tests carried out (oxidation and incubation tests) showed that the wastes constitute a potential source of sulfated acid drainage that will also affect the soil and groundwater even more in the future. The process by which the soil becomes acidic and releases significant amounts of sulfates in solution to the groundwater is associated with the fact that native sulfur reacts with rainwater under oxidizing conditions in the unsaturated zone. The interaction with the rainwater causes the oxidation of the native sulfur releasing protons and sulfates, which reach the groundwater through the infiltration water process, generating the acidification of the environment.

Identifying the waste spatial distribution and the area affected by the acid drainage generated by the waste, and defining whether the groundwater is affected due to infiltration of soluble compounds such as sulfates through rainwater, is essential when defining remediation and/or mitigation guidelines. The monitoring data obtained could help to find remediation options and is useful data for the management of environmental liabilities, which constitute a problem of environmental relevance and whose regulations for management and mitigation are still a controversial issue.

Acknowledgements L. Santucci acknowledges a postdoctoral fellowship and E. Carol is member of CIC in the Consejo Nacional de Investigaciones Científicas y Técnicas (National Council for Scientific and Technological Research).

Data and materials availability The datasets used and/or analyzed during the current study are available from the corresponding author on reasonable request.

Author contribution AG: field surveys and water and sediments sampling in the petrochemical center area, chemical analysis of water and sediments samples, investigation and writing the manuscript. SL: field surveys and water and sediments sampling in the petrochemical center area, chemical analysis of water and sediments samples. Interpretation of geochemical data, investigation and writing the manuscript. CE: field surveys and water and sediments sampling in the petrochemical center area. Interpretation of geochemical data, investigation, writing the manuscript and funding acquisition.

Funding The authors received funding from Agencia Nacional de Promoción Científica y Tecnológica (National Agency for Scientific and Technological Promotion) and the Universidad Nacional de La Plata (National University of La Plata) of Argentina by means of their grants PICT 2016-0539 and N906 respectively.

Declarations

Ethics approval The submitted paper meets the ethical standards set by Environmental Science and Pollution Research.

Consent to participate Not applicable.

Consent to publication All authors agreed with the submission and approved the publication.

Code availability Not applicable.

Conflict of interest The authors declare no competing interests.

References

Ainchil, J., & Kruse, E. (2002). Características hidrogeológicas de la Planicie Costera en el Noreste de La Plata, Buenos Aires, Argentina. *Groundwater and Human Development. Mar del Plata (Argentina)*, 606–612.

APHA. (2017). *Standard Methods for the Examination of Water and Wastewater* (23rd ed.). Washington D.C.: American Public Health Association.

Bigham, J. M., & Nordstrom, D. K. (2000). Iron and aluminum hydroxysulfates from acid sulfate waters. *Reviews in Mineralogy and Geochemistry, 40*(1), 351–403.

van Breemen, N. (1973). *Soil forming processes in acid sulphate soils. Proceedings of the International Symposium in Acid Sulphate Soils. 13–20 August 1972, Wageningen, The Netherlands* (pp. 66–129). Wageningen, The Netherlands: Int. Inst. for Land Reclamation and Improvement.

Campbell, F. T., Pfefferkorn, R., & Rounsaville, J. F. (1993). *Sulfuric acid and sulfur trioxide, Ullman's Encyclopedia of Industrial Chemistry* (5a. edicion ed.pp. 635–699). Deerfield Beach, Florida, USA: Weinheim- VCH.

Carol, E. S., Kruse, E. E., Laurencena, P. C., Rojo, A., & Deluchi, M. H. (2012). Ionic exchange in groundwater hydrochemical evolution. Study case: the drainage basin of El Pescado creek

(Buenos Aires province, Argentina). *Environmental Earth Sciences, 65*(2), 421–428.

Carol, E., del Pilar Alvarez, M., Idaszkin, Y. L., & Santucci, L. (2019). Salinization and plant zonation in Argentinian salt marshes: Natural vs. anthropic factors. *Journal of Marine Systems, 193*, 74–83.

Corfield, J. (2000). The effects of acid sulphate run-off on a subtidal estuarine macrobenthiccommunity in the Richmond River, NSW, Australia. ICES (Int. Counc. Explor. Sea). *Journal of Marine Science, 57*(5), 1517–1523.

Costa, M. C., & Duarte, J. C. (2005). Bioremediation of acid mine drainage using acidic soil and organic wastes for promoting sulphate-reducing bacteria activity on a column reactor. *Water, Air, and Soil Pollution, 165*(1-4), 325–345.

Costa, M. C., Martins, M., Jesus, C., & Duarte, J. C. (2008). Treatment of acid mine drainage by sulphate-reducing bacteria using low cost matrices. *Water, Air, and Soil Pollution, 189*(1), 149–162.

Costanza, R., Kemp, W. M., & Boynton, W. R. (1993). Predictability, scale and biodiversity in coastal and estuarine ecosystems: implications for management. *Ambio, 22*, 88–96.

Crockford, R. H., & Willett, I. R. (1995). Drying and oxidation effects on the magnetic properties of sulfidic material during oxidation. *Soil Research, 33*(1), 19–29.

De Sousa, C. (2001). Contaminated sites: the Canadian situation in an international context. *Journal of Environmental Management, 62*(2), 131e154.

Delgado, J., Barba-Brioso, C., Ayala, D., Boski, T., Torres, S., Calderón, E., & López, F. (2019). Remediation experiment of Ecuadorian acid mine drainage: geochemical models of dissolved species and secondary minerals saturation. *Environmental Science and Pollution Research, 26*(34), 34854–34872.

Dent, D. L. (1986). *Acid sulphate soils: a baseline for research and development.* ILRI Publ. 39, Wageningen.

Devasahayam, S. (2006). Chemistry of acid production in black coal mine washery wastes. *International Journal of Mineral Processing, 79*(1), 1–8.

Diao, M., Huisman, J., & Muyzer, G. (2018). Spatio-temporal dynamics of sulfur bacteria during oxic–anoxic regime shifts in a seasonally stratified lake. *FEMS Microbiology Ecology, 94*(4), fiy040.

Ferreira, R. A., Pereira, M. F., Magalhães, J. P., Maurício, A. M., Caçador, I., & Martins-Dias, S. (2020). Assessing local acid mine drainage impacts on natural regeneration-revegetation of São Domingos mine (Portugal) using a mineralogical, biochemical and textural approach. *Science of the Total Environment, 142825*.

Frigaard, N. U., & Dahl, C. (2008). Sulfur metabolism in phototrophic sulfur bacteria. *Advances in Microbial Physiology, 54*, 103–200.

García, M. A., Chimenos, J. M., Fernández, A. I., Miralles, L., Segarra, M., & Espiell, F. (2004). Low-grade MgO used to stabilize heavy metals in highly contaminated soils. *Chemosphere, 56*(5), 481e491.

Gerritse, R. G., Barber, C., & Adeney, J. A. (1990). *The impact of residential urban areas on groundwater quality: Swan Coastal Plain, Western Australia* (Vol. 3).

Idaszkin, Y. L., Carol, E., & Alvarez, M. (2017). Mechanism of removal and retention of heavy metals from the acid mine drainage to coastal wetland in the Patagonian marsh. *Chemosphere, 183*, 361–370.

Jennings, S. R., Dollhopf, D. J., & Inskeep, W. P. (2000). Acid production from sulfide minerals using hydrogen peroxide weathering. *Applied Geochemistry, 15*(2), 235–243.

Konner, Z. S. (1993). Comparative study of adsorption behaviour of copper, lead, and zinc onto goethite in aqueous system. *Environmental Geology, 21*, 242–250.

Konsten, C. J. M., Brinkman, R., & Andriesse, W. (1988). A field laboratory method to determine total potential and actual acidity in acid sulphate soils. In *Selected papers of the Dakar symposium on acid sulphate soils: Dakar, Senegal, January 1986* (pp. 106–134).

Lecomte, K. L., Maza, S. N., Collo, G., Sarmiento, A. M., & Depetris, P. J. (2017). Geochemical behavior of an acid drainage system: the case of the Amarillo River, Famatina (La Rioja, Argentina). *Environmental Science and Pollution Research, 24*(2), 1630–1647.

Lin, Z. (1997). Mineralogical and chemical characterization of wastes from the sulfuric acid industry in Falun, Sweden. *Environmental Geology, 30*(3-4), 152–162.

Lin, Z., & Quvarfort, U. (1996). Predicting the mobility of Zn, Fe, Cu, Pb, Cd from roasted sulfide (pyrite) residues—a case study of wastes from the sulfuric acid industry in Sweden. *Waste Management, 16*(8), 671–681.

Ljung, K., Maley, F., Cook, A., & Weinstein, P. (2009). Acid sulphate soils and human health-A millenium ecosystem assessment. *Environment International, 35*(8), 1234–1242.

Logan, W., & Nicholson, R. (1998). Origin of dissolved groundwater sulphate in coastal plain sediments of the Rio de la Plata, Eastern Argentina. *Aquatic-Geochemistry, 3*, 305–328.

Logan, W. S., Auge, M. P., & Panarello, H. O. (1999). Bicarbonate, sulfate, and chloride water in a shallow, clastic-dominated coastal flow system, Argentina. *Groundwater, 37*, 287–295.

Lövgren, L., Sjöberg, S., & Schindler, P. W. (1990). Acid/base reactions and Al (III) complexation at the surface of goethite. *Geochimica et Cosmochimica Acta, 54*(5), 1301–1306.

Ludwig, B., Prenzel, J., & Obermann, P. (2001). Modelling ion composition in seepage water from a column experiment with an open cut coal mine sediment. *Journal of Geochemical Exploration, 73*(2), 87–95.

Meire, P., Ysebaert, T., Van Damme, S., Van den Bergh, E., Maris, T., & Struyf, E. (2005). The Scheldt estuary: a description of a changing ecosystem. *Hydrobiologia, 540*, 1–11.

Müller, H. (1994). Sulfuric acid and sulfur trioxide. *Ullmann's Encyclopedia of Industrial Chemistry, 35*, 141–211.

NF ISO 10390. (1994). *Soil quality - determination of pH*. Geneva, Switzerland: International Organization for standardization 5p.

Nieto, J. M., Sarmiento, A. M., Canovas, C. R., Olias, M., & Ayora, C. (2013). Acid mine drainage in the Iberian Pyrite Belt: 1. Hydrochemical characteristics and pollutant load of the Tinto and Odiel rivers. *Environmental Science and Pollution Research, 20*(11), 7509–7519.

Nieva, N. E., Borgnino, L., Locati, F., & García, M. G. (2016). Mineralogical control on arsenic release during sediment–water interaction in abandoned mine wastes from the Argentina Puna. *Science of the Total Environment, 550*, 1141–1151.

Nieva, N. E., Borgnino, L., & García, M. G. (2018). Long term metal release and acid generation in abandoned mine wastes containing metal-sulphides. *Environmental Pollution, 242*, 264–276.

Nordstrom, D. (1982). Aqueous pyrite oxidation and the consequent formation of secondary iron minerals. *Acid Sulfate Weathering, 10*, 37–56.

Pons, L. J. (1973). Outline of the genesis, characteristics, classification and improvement of acid sulphate soils. In *Proceedings of the 1972 (Wageningen, Netherlands) International Acid Sulphate Soils Symposium* (Vol. 1, pp. 3–27).

Pradhan, B. (2014). Corrosion behavior of steel reinforcement in concrete exposed to composite chloride–sulfate environment. *Construction and Building Materials, 72*, 398–410.

QGIS.org. (2020). *QGIS Development Team.* QGIS Geographic Information System. Open Source Geospatial Foundation Project (http://www.qgis.org/es/site/).

Rennenberg, H. (1984). The fate of excess sulfur in higher plants. *Annual Review of Plant Physiology, 35*(1), 121–153.

Rezaie, B., & Anderson, A. (2020). Sustainable resolutions for environmental threat of the acid mine drainage. *Science of the Total Environment, 717*, 137211.

Santucci, L. (2020). Dinámica de la relación agua superficial - agua subterránea como condicionante de los procesos geoquímicos que regulan la calidad del agua. Tesis doctoral. Universidad Nacional de La Plata.

Santucci, L., Carol, E., & Kruse, E. (2016). Identification of palaeo-seawater intrusion in groundwater using minor ions in a semi-confined aquifer of the Río de la Plata littoral (Argentina). *Science of the Total Environment, 566*, 1640–1648.

Santucci, L., Carol, E., Borzi, G., & García, M. G. (2017). Hydrogeochemical and isotopic signature of surface and groundwater in a highly industrialized sector of the Rio de la Plata coastal plain (Argentina). *Marine Pollution Bulletin, 120*(1-2), 387–395.

Santucci, L., Carol, E., & Tanjal, C. (2018). Industrial waste as a source of surface and groundwater pollution for more than half a century in a sector of the Río de la Plata coastal plain (Argentina). *Chemosphere, 206*, 727–735.

Schmidt, A., & Jäger, K. (1992). Open questions about sulfur metabolism in plants. *Annual Review of Plant Biology, 43*(1), 325–349.

Schnack, E., Isla, F., De Francesco, F., Fucks, E. (2005). Estratigrafía del Cuaternario marino tardío en la provincia de Buenos Aires. XVI Congreso Geológico Argentino, Relatorio 159–182, La Plata.

Schwertmann, U., & Fitzpatrick, R. W. (1993). Iron minerals in surface environments. *Catena Supplement, 21*, 7–7.

Shaheen, F., & Pradhan, B. (2017). Influence of sulfate ion and associated cation type on steel reinforcement corrosion in concrete powder aqueous solution in the presence of chloride ions. *Cement and Concrete Research, 91*, 73–86.

Sweerts, J. P. R., De Beer, D., Nielsen, L. P., Verdouw, H., Van den Heuvel, J. C., Cohen, Y., & Cappenberg, T. E. (1990). Denitrification by sulphur oxidizing Beggiatoa spp. mats on freshwater sediments. *Nature, 344*(6268), 762–763.

Tugrul, N., Derun, E. M., Piskin, M., & Piskin, S. (2003). Evaluation of pyrite ash wastes obtained by the sulfuric acid production industry. In *Proceedings of the 8th International Conference on Environmental Science and Technology, Lemmos Island, Vol. A, Greece* (pp. 918–925).

Turner, L. J., & Kramer, J. R. (1992). Irreversibility of sulfate sorption on goethite and hematite. *Water, Air, and Soil Pollution, 63*(1-2), 23–32.

Ward, N. J., Sullivan, L. A., & Bush, R. T. (2004a). Soil pH, oxygen availability and the rate of sulfide oxidation in acid sulfate soil materials: implications for environmental hazard assessment. *Australian Journal of Soil Research, 42*, 509–514.

Ward, N. J., Sullivan, L. A., Fyfe, D. M., Bush, R. T., & Ferguson, A. J. P. (2004b). The process of sulfide oxidation in some acid sulfate soil materials. *Australian Journal of Soil Research, 42*, 29–37.

Watling, K. M., Ahern, C. R., & Hey, K. M. (2004). *1 Acid sulfate soil field pH tests. Acid Sulfate Soils Laboratory Methods Guidelines* (pp. H1-1–H1-4). Queensland, Australia: Queensland Department of Natural Resources, Mines and Energy, Indooroopilly.

Yang, C., Chen, Y., Li, C., Chang, X., & Wu, Y. (2009). Trace element transformations and partitioning during the roasting of pyrite ores in the sulfuric acid industry. *Journal of Hazardous Materials, 167*(1-3), 835–845.

Zhou, C., Zhu, Z., Wang, Z., & Qiu, H. (2018). Deterioration of concrete fracture toughness and elastic modulus under simulated acid-sulfate environment. *Construction and Building Materials, 176*, 490–499.